Carbohydrate Polymers 98 (2013) 644–649

Contents lists available at SciVerse ScienceDirect

Carbohydrate Polymers

journal homepage: www.elsevier.com/locate/carbpol

On the weak dependence of water diffusivity on the degree of hydrophobicity of acetylated hydroxypropyl xylan

Diwen Zhou, Fatemeh Bayati, Phillip Choi*

Department of Chemical and Materials Engineering, University of Alberta, Edmonton, AB, Canada T6G 2V4

ARTICLE INFO

Article history:
Received 22 April 2013
Received in revised form 7 June 2013
Accepted 19 June 2013
Available online 26 June 2013

Keywords:
Water diffusivity
Xylans
Molecular dynamics simulation
Swelling
Hydrogen bonds

ABSTRACT

We used molecular dynamics (MD) simulation to study the diffusion of water at low concentrations in a series of chemically modified xylans, a major hemicellulose, including hydroxypropyl xylan (HPX) and acetoxypropyl xylan (APX) which is essentially acetylated HPX, with different degrees of acetylation (i.e., different degrees of hydrophobicity) at 400 K, a temperature well above the glass transition temperatures of the materials. We used one HPX and three APX models. The three APX models were constructed using the HPX model by substituting 1, 2 or 3 hydroxyl moieties on its repeating units, respectively.

The simulation results showed that the diffusivity of water at low concentrations in the chemically modified xylans decreased slightly (~20%) from HPX to APX with 3 acetylated hydroxyl moieties, a trend that has been experimentally observed for xylans and other cellulosic type materials. Further data analysis shows that acetylation decreases the ability of the xylan to form hydrogen bonds with water and its degree of swelling. And these two factors exert opposite effects on the diffusivity of water. In particular, the first factor increases the mobility (lower activation energy) of the water molecules, while the second factor reduces the free volumes available for diffusion, thereby decreasing the water mobility. This finding implies that it is not likely to obtain orders of magnitude change to the water diffusivity simply by the acetylation of all hydroxyl moieties on xylan. The high degree of swelling observed for HPX compared to those of APXs is attributed to the fact that many hydrogen bonds in HPX are broken by water. It is interesting to note that water in most of the hydrogen bonds formed between water and xylans acted as hydrogen bond acceptors rather than donors.

1. Introduction

The sustainability issue of using synthetic polymers is of a major concern in today's society as they are derived from non-renewable resources and are being non-biodegradable. As a result, there has been an increasing interest in developing biopolymers from renewable resources to replace synthetic polymers (Gonzalez, Santos, & Parajo, 2011). In particular, there is an extensive effort on modifying natural polymers from various types of plants for such a purpose.

Hemicelluloses are the second abundant component in wood and plants after cellulose. Unlike cellulose, hemicelluloses are hetero-polysaccharides that contain different types of sugar units with different substituents arranged at different proportions. They are short-branch, amorphous polymers with degrees of polymerization around 50–300. Hemicelluloses are hydrophilic and soluble in water (Cordeiro, Gouveia, Moraes, & Amico, 2011; Sun, Sun, & Tomkinson, 2004).

Native or modified forms of hemicelluloses are an important renewable source of biopolymers which can be used in different areas like food and non-food packaging materials, coatings and matrix for bio-based composites (Hansen & Plackett, 2008; Mikkonen & Tenkanen, 2012). They show good properties for making adhesives, thickeners, stabilizers, decorative paints, film formers, hydrogels, and emulsifiers (Cordeiro et al., 2011; Peura, Karppinen, Soovre, Salmi, & Tenkanen, 2008; Phan et al., 2002; Pohjanlehto, Setala, Kammiovirta, & Harlin, 2011; Saxena, Elder, & Ragauskas, 2008; Stepan, Hoije, Schols, de Waard, & Arabinose, 2012).

Being the principal component of hemicelluloses in many plants, xylan constitutes 20–35% of the total dry weight of plants. Xylan, with xylose, a key sugar unit in xylan, content of 60–70%, is one of the highly branched, low molecular weight, non-cellulosic, non-crystalline hetero-polysaccharides. Xylan is now mostly used for conversion process to xylose, xylitol and furfural. Production of xylan derivatives is advantageous as they are easy to process but also biodegradable and environmentally degradable (Ebringerova

* Corresponding author. Present address: Department of Chemical and Materials Engineering, University of Alberta, 9107 116 street, Edmonton, AB, Canada T6G 2V4. Tel.: +1 780 4929018.
E-mail address: phillip.choi@ualberta.ca (P. Choi).

0144-8617/$ – see front matter © 2013 Elsevier Ltd. All rights reserved.
http://dx.doi.org/10.1016/j.carbpol.2013.06.025

& Heinze, 2000; Glasser, Jain, & Sjostedt, 1995; Jain, Sjostedt, & Glasser, 2000).

Derivatizing hydroxyl groups of xylan to new chemical groups would yield a film forming material that can be used in applications such as edible and non-edible films and coatings (Fundador, Enomoto-Roger, TakemurA, & Iwata, 2012; Goksu, Karamanlioglu, Bakir, Yilmaz, & Yilmazer, 2007; Hartman, Albertsson, Lindblad, & Sjoberg, 2006; Peroval, Debeaufort, Despre, & Voillley, 2002), hydrogels (Gabrielii & Gatenholm, 1998; Pohjanlehto et al., 2011; Tanodekaew, Channasanon, & Uppanan, 2006; Voepel, Edlund, & Albertsson, 2009), biodegradable plastics and plasticizers (Rauschenberg, Dhara, Palmer, & Glasser, 1990; Shaikh, Pandare, Nair, & Varma, 2009). Chemical modification of xylan by substituting xylan's hydroxyl group by alkoxy or acetoxy substitutes helps induce its solubility in water or organic solvents, respectively. Hydroxypropyl cellulose and starch have been found in many applications in industry due to their water solubility. However, hydroxypropyl xylan (HPX) with similar properties has remained obscure. Among the xylan derivatives, only xylan acetate has been studied (Jain et al., 2000).

HPX with degrees of substitution of 0.2–0.5 are water-soluble and can form transparent and tough films that have the potential to be used in food packaging (Jain et al., 2000). In order to be used in such application (i.e., to protect food from contamination and deterioration), it is important for the film to act as oxygen and moisture barrier. Due to hygroscopic nature of hemicelluloses, they are poor moisture barriers. Increasing hydrophobicity by coating the surface of film with a water barrier material, addition of hydrophobic compounds or chemical modification (e.g., acetylation, grafting, etc.) may solve this problem (Escalante et al., 2012). Although there have been many studies for improving barrier properties of HPX, as quantified by water vapor transmission rate (WVTR) and water vapor permeability (WVP), not all of them have comparable results with current commercial products such as low-density polyethylene (Hansen & Plackett, 2008). There are still concerns whether improving hydrophobicity of HPX would decreases WVTR or not (Pan, Xiao, & Song, 2013). According to Pan et al. (2013), WVTR is insensitive to the degree of hydrophobicity of HPX. Gennadios, Weller, and Testin (1993) were able to improve hydrophobicity of gluten-based films using hydrolyzed keratin and mineral oil but the WVTR reduction was only 23–25%.

The counter intuitive experimental results led to the speculation that during the hydrophobization of HPX, the solvent used causes the HPX film to swell. If all of the swelling is not reversible, the extra free volume introduced in the polymer would increase the mobility of water. In addition, the residue solvent may act as a plasticizer, enhancing the mobility of the HPX molecules (Ahlen, 1969). All of such reasons make hydrophobization an inefficiency approach to improve the barrier properties of HPX films. In this regard, we carried out molecular dynamics simulation on a series of chemically modified xylans (one HPX and three acetoxypropyl xylan (APX) with different degrees of acetylation of HPX) to discern the molecular mechanisms that lead to the observed insensitivity of water diffusivity to the degree of hydrophobicity of the materials.

2. Models and simulation method

In this work, the structure of the model HPX resembles to that of a film forming HPX that possesses a linear structure and is a hydrophilic, water-swollen polymer (see Fig. 1). The molecular weight of model HPX is 4404 (10 repeating units).

To increase the hydrophobicity of the polymer, we substituted 1, 2 or 3 hydroxyl moieties on the side chains attached to the repeating unit of HPX with acetic acid to construct three different model APXs (see Fig. 2) with different degrees of acetylation (hydrophobicity).

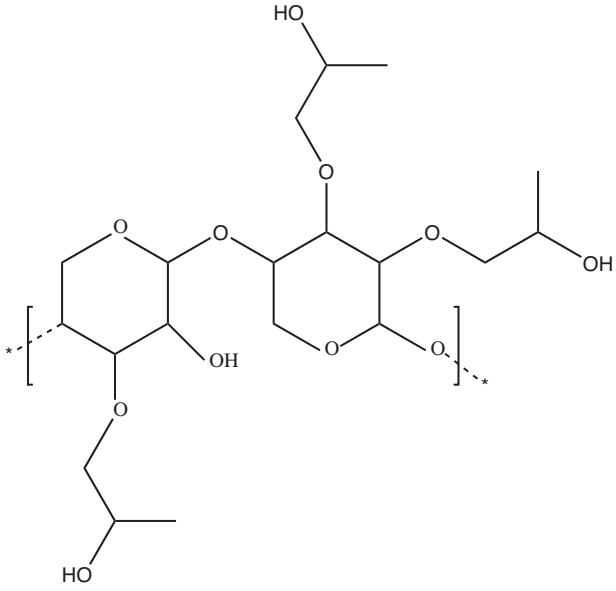

Fig. 1. Structure of the repeating unit of HPX.

The molecular weights of APX1, APX2 and APX3 are 4824, 5244 and 5664, respectively (all APX chains contained 10 repeating units).

Only the amorphous phase of the HPX and APXs was interested in the present work. The amorphous phase was generated by a commercial software Materials Studio version 5.0 based upon the procedure described by Theodorou and Suter (1985), a procedure that has been extensively used to generate amorphous phase of polymers. Nonetheless, when we constructed the initial amorphous configurations, we used a hard core radius to each atom equal to 0.3 times of their van der Waals radius to avoid hard overlaps. This would, in turn, avoid the high-energy structures towards the end of the amorphous model construction process. To mimic the bulk amorphous state of these polymers, one or two chains were used in a cubic box with an initial density as 1×10^3 kg/m^3 and subjected to three-dimensional periodic boundary condition. Once the pure polymer systems were set up, energy minimization was carried out with the steepest descent method. The systems were subjected to isothernal–isobaric (i.e., NPT) molecular dynamics (MD) simulation to equilibrate their density to 1.16×10^3 kg/m^3 (HPX), 1.14×10^3 kg/m^3 (APX1), 1.14×10^3 kg/m^3 (APX2) and 1.12×10^3 kg/m^3 (APX3), respectively. Here, the NPT equilibration temperature was set at 400 K, a temperature significantly higher than the glass transition temperatures of the xylans and the pressure was set at 1 atm. We used Nose–Hoover coupling (Hoover, 1985; Nose, 1984) to control the temperature and Parrinello–Rahman approach (Nose & Klein, 1983; Parrinello & Rahman, 1981) to control the pressure. After that, we inserted water molecules into each system and the energy minimization was carried out again.

For each chemically modified xylan model, a total of 5 systems, corresponding of five water concentrations, were generated (see Table 1). And for each system, 10 NPT MD simulations with different initial positions of water molecules were carried out at the same temperature (400 K) and pressure (1 atm) to improve the statistics. Each simulation was carried out for 12 ns and the time step Δt was 1 fs. We used the leap-frog algorithm (Hockney, Goel, & Eastwood, 1974) to integrate the Newtonian equations of motion.

To calculate the diffusion coefficients of water in the polymers, we used the Einstein's equation:

$$D = \frac{1}{6}\frac{d(\langle(1/N)\sum(\vec{r}_i(t) - \vec{r}_i(0))^2\rangle)}{dt} \quad (1)$$

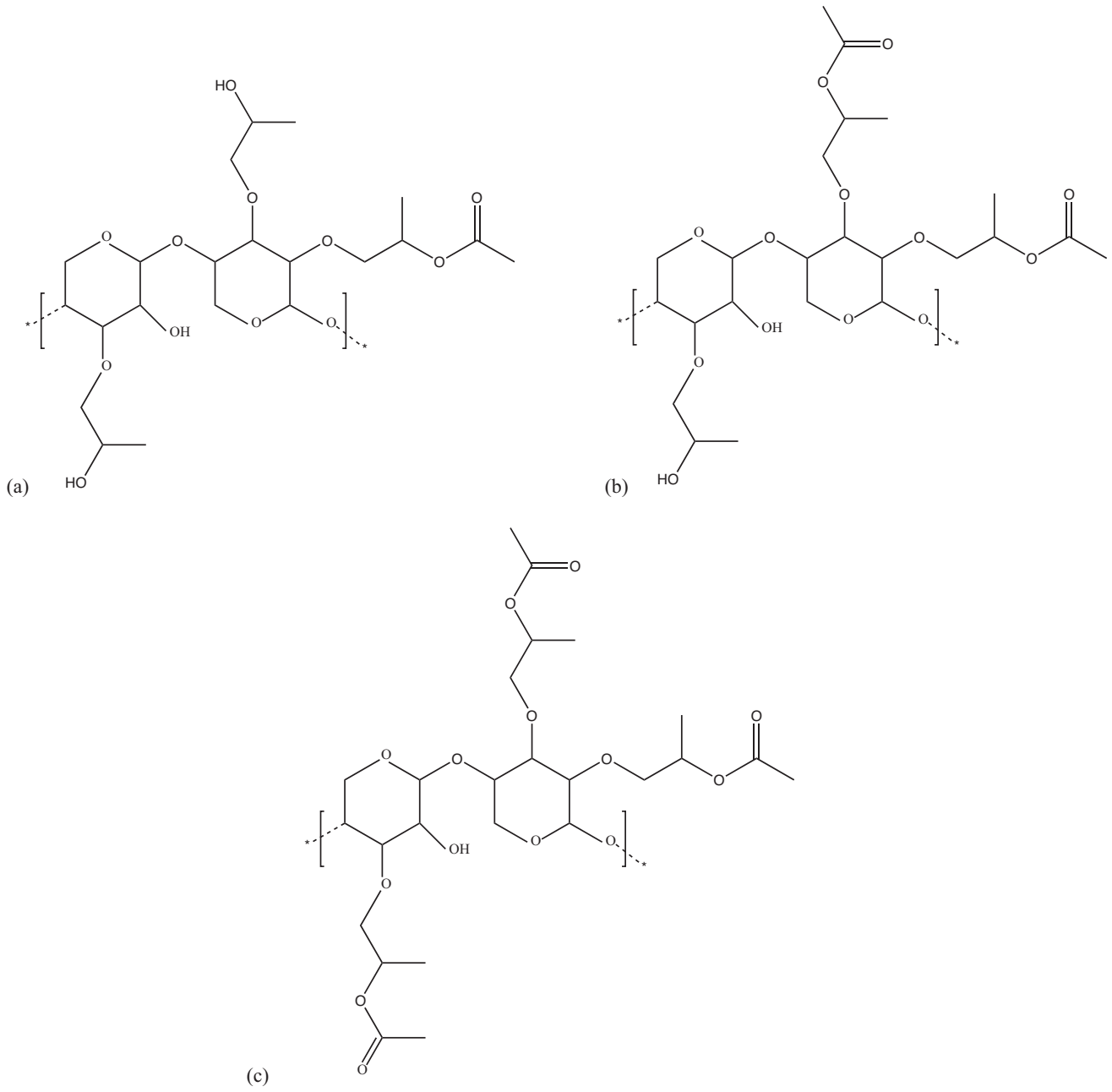

Fig. 2. Structure of APX1 (a), APX2 (b) and APX3 (c).

Here $\langle (1/N)\sum(\vec{r}_i(t)-\vec{r}_i(0))^2\rangle$ is the mean-square displacement (MSD) of the water molecules.

All MD calculations were performed using the Gromacs package. Here, we used the force field called GROMOS96 a5. This force field is a condensed-phase force field and suitable for systems composed of organic liquids, solutions and crystals. The GROMOS force field has been developed by W. F. van Gunsteren and co-workers since 1978 (Scott et al., 1999). GROMOS96 has been able to reproduce a variety of properties of systems containing water and polymer (Daura, Mark, & van Gunsteren, 1998).

In the GROMOS96 force field, there are two types of potentials describing the interaction between particles. One is the bond potential while the other is non-bond potential. The bond potential is described by the following equation:

$$(r) = \Sigma\frac{1}{4}K_1[b_n^2 - b_{n0}^2]^2 + \Sigma\frac{1}{2}K_2[cos\theta_n - cos\theta_{n0}]^2 + \Sigma\frac{1}{2}K_3[\xi_n - \xi_{n0}]^2 + \Sigma K_4[1 + cos(\delta_n)cos(m_n\varphi_n)] \quad (2)$$

This potential has four terms. K_1–K_4 are the four force constants. The first term specifies the force originating from the change of the covalent bond length. The second term originates from the angle bending between two neighboring bonds. The third term corresponds to the force coming form the change of improper dihedral angle and the fourth term indicates the torsion of dihedral angle.

The non-bond potential could be specified by the following equation:

$$V(r) = \Sigma \left\{ \left[\frac{C12_{ij}}{r_{ij}^6} - C6_{ij} \right] \frac{1}{r_{ij}^6} + \frac{q_i q_j}{4\pi\varepsilon_0\varepsilon_1} \frac{1}{r_{ij}} + V^{RF}(r_{ij}, q_i, q_j, R_{RF}, \varepsilon_1, \varepsilon_2, \kappa) \right\} \quad (3)$$

This potential will be applied to all particle pairs without bond potentials. Also a cut off distance 1 nm was used to reduce computational efforts. The non-bond potential includes three terms. The first term denotes the van der Waals interaction. And $C12_{ij}$ and $C6_{ij}$ are the van der Waals interaction constants. The second term corresponds to the electric state potential and q_i and q_j are the charges on the particles. The third term is the electrostatic interactions by Poisson–Boltzmann generalized reaction field term. For the water model, we used the SPCE model, as it is able to reproduce the diffusion property of water in the bulk very well (Mark & Nilsson, 2001).

3. Results and discussion

To illustrate how diffusion coefficient is calculated from a molecular dynamics simulation trajectory, we use System 2 as an example. Fig. 3 shows the MSD of water molecules in System 2 over a period of 12 ns. According to Eq. (1), the corresponding diffusion coefficient is equal to the slope of the regressing line fitted through the linear portion of the MSD versus time curve (the so-called Einstein diffusion regime, 4–11 ns in this case). It should be noted that when the diffusion data is plotted in a log-log plot, the resultant regressing line should have a slop of 1 and the intercept yields the diffusion coefficient. In fact, this is the case for all systems depicted in Table 1.

Fig. 4 summarizes the calculated diffusion coefficients for all 20 systems. Figs. 5 and 6 give the corresponding K values and the mean number of polymer–water hydrogen bonds (HB), respectively. It should be noted that each data point corresponds to a mean of the time averages of 10 MD simulations using different initial positions of the water molecules but subjected to the same simulation conditions. Here, K is defined in the following equation:

$$K = \frac{(V - V_0)/V_0}{(m - m_0)/m} \quad (4)$$

where V_0 and V are the volumes of xylan in the absence and presence of water and m_0 and m are the corresponding mass. In other words, K is the fractional volume change normalized to the weight fraction of water. Larger K value signifies higher degree of swelling.

Fig. 4 clearly shows that D exhibits a significant drop over the water concentration range from 1.0% to 3.0% for all xylan models and is more or less insensitive to the water concentration once it is above 3%. The water concentration dependence of D reported here is similar to that of a polyether-based polyurethane seen in our previous work (Zhou & Choi, 2012), in which the observed concentration dependence of D was found to be attributed to the decreasing degree of swelling of the polymer and increasing number of polymer–water hydrogen bonds when the water concentration is increased. Analysis of the present data indicates that

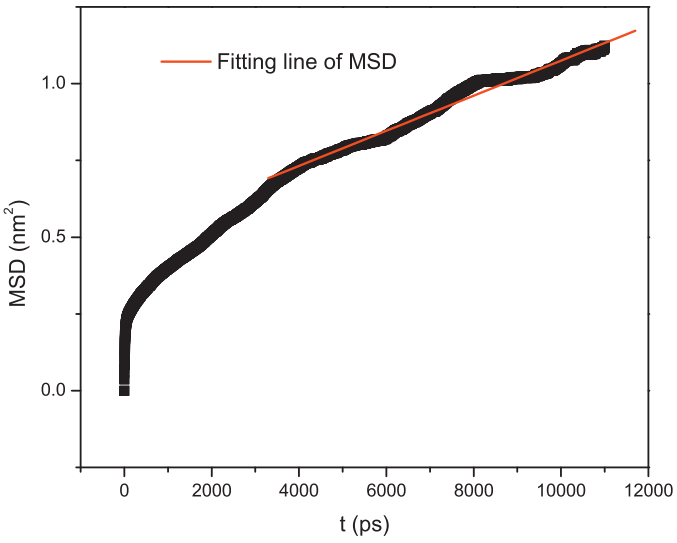

Fig. 3. The MSD of all water molecules versus time for System 2 over a period of 12 ns.

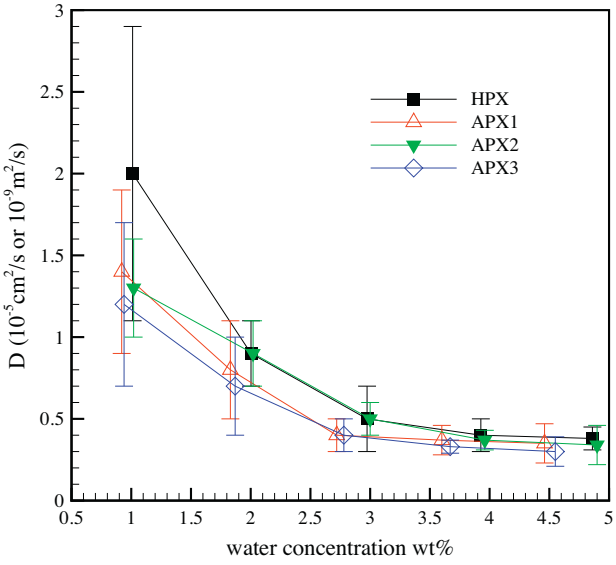

Fig. 4. Calculated diffusion coefficient (D) for various water concentrations in different xylans

Table 1
Model systems at various water concentrations.

System	Polymer type	Number of polymer chains	Number of water molecules	Water concentration wt%
1	HPX	2	5	1.01%
2	HPX	2	10	2.00%
3	HPX	2	15	2.97%
4	HPX	2	20	3.93%
5	HPX	2	25	4.86%
6	APX1	2	5	0.92%
7	APX1	2	10	1.83%
8	APX1	2	15	2.72%
9	APX1	2	20	3.60%
10	APX1	2	25	4.46%
11	APX2	1	3	1.02%
12	APX2	1	6	2.02%
13	APX2	1	9	3.00%
14	APX2	1	12	3.96%
15	APX2	1	15	4.90%
16	APX3	1	3	0.94%
17	APX3	1	6	1.87%
18	APX3	1	9	2.78%
19	APX3	1	12	3.67%
20	APX3	1	15	4.55%

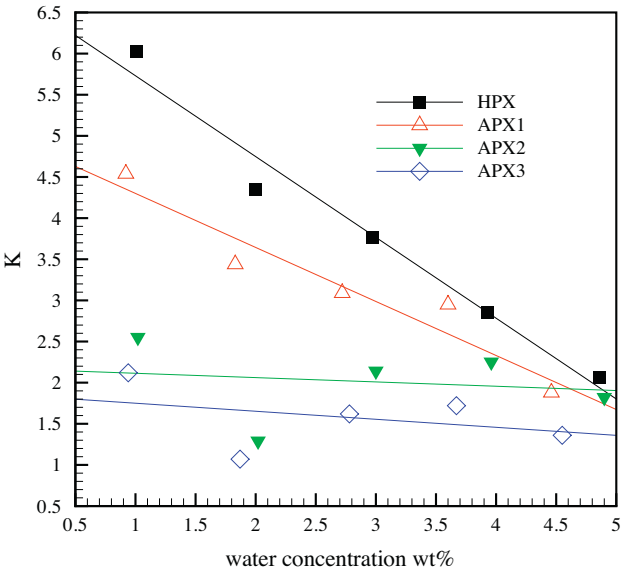

Fig. 5. *K* value of xylans at various water concentrations.

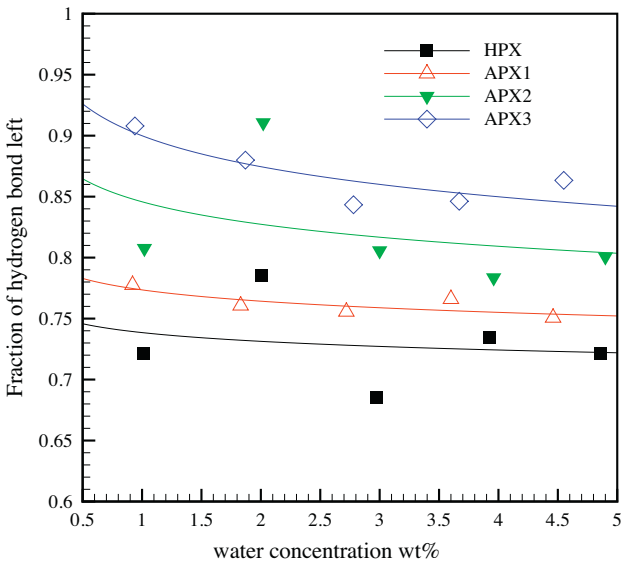

Fig. 7. The water concentration dependence of the fraction of polymer–polymer hydrogen bonds remained in xylans.

the same explanations also apply to xylans. Although the degree of swelling of both polyether-based polyurethane and xylans, as characterized by *K*, exhibits a negative dependence on the water concentration, the dependence of former is non-linear while the latter is more or less linear. The difference may be due to the fact that the polyether-based polyurethane contains only hydrogen bond donors while xylans contain both hydrogen bond donors and acceptors. In other words, polyether-based polyurethane cannot form polymer–polymer hydrogen bonds while xylans can. Nonetheless, the negative water concentration dependence of *K* means that there is less free volumes available for the diffusion of water, thereby decreasing the resultant D.

A note worthy point about Fig. 5 is that the differences between their *K* values become smaller as the water concentration increases. This is attributed to two factors. First, at low water concentrations, there are higher chances that the polymer–polymer hydrogen bonds are broken for HPX compared to APXs. This is because there are more polymer–polymer hydrogen bonds to be broken by water molecules in the case of HPX (4 hydrogen bond donors and 6 hydrogen bond acceptors per repeating unit) compared to APX3 (1 hydrogen bond donor and 12 hydrogen bond acceptors per repeating unit). Such difference would diminish as water concentration is increased. Fig. 7 plots the fractions of polymer–polymer hydrogen bonds remained in the xylans. Obviously, the fraction of polymer–polymer hydrogen bonds remained in HPX is much lower than the other APXs. It should be noted that hydrogen bonds are short-range interaction that leads to close packaging of the polymer chains. Breaking polymer–polymer hydrogen bonds leads to swelling. The second factor is about the definition of *K* as it is normalized to the weight faction of water. Therefore, it is expected that the difference in *K* will decrease as water concentration is increased.

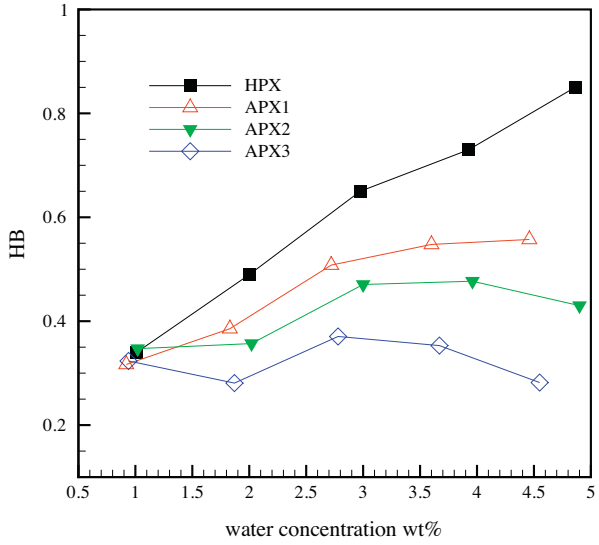

Fig. 6. HB value of xylans at various water concentrations.

As can be seen in Fig. 6, the number of polymer–water hydrogen bonds increases considerably with increasing water concentration for HPX but not for APXs. It should be noted that APXs contain a high number of hydrogen bond acceptors. This suggests that water acts as hydrogen bond acceptors, rather than donors in xylans.

The most interesting feature of Fig. 4 is that *D* shows a weak negative dependence on the degree of acetylation (i.e., hydrophobicity) except at 1% water concentration. This is somewhat unexpected. However, this trend has also been observed experimentally as mentioned in the introduction. It is worth noting that at 1% water concentration, the diffusion coefficient of water molecules in HPX (the least hydrophobic xylan) is about 40–70% higher than those of the APXs. It should be pointed out that there are also large uncertainties associated with the corresponding data.

As mentioned earlier, the degree of swelling and the polymer–water hydrogen bonds are the two factors that control the diffusivity of water. It seems that these factors can also be used to explain the insensitivity of water diffusivity to the hydrophobicity of xylan. As shown in Fig. 5, at a given water concentration, it is obvious that the degree of swelling decreases as the hydrophobicity of xylan increases. This means that there is less free volume available for the diffusion of water in xylans with high degrees of hydrophobicity, thereby lowering the corresponding diffusion coefficients. On the other hand, the number of polymer–water hydrogen bonds decreases, thereby increasing the mobility of the water molecules. Here, hydrogen bonds increase the activation energy for the diffusion motion. Taking 3% concentration as an example, the K value of HPX (least hydrophobic) is about 2 times of that of APX3 (most hydrophobic) while the number of polymer–water hydrogen bonds

of HPX is about 2 times of that of APX3. Since the effects offset each other, the diffusion coefficient of water in APX3 is only slightly lower than that of HPX.

4. Conclusion

We studied the effect of the degree of hydrophobicity of a series of xylans on the water diffusivity using molecular dynamics simulation. In particular, we simulated hydroxylpropyl xylan (HPX) and acetopropyl xylan (APX) with different degrees of acetylation (i.e., different degrees of hydrophobicity). Simulation results showed the same trend as observed in experiment that water diffusivity exhibits a weak negative dependence on the degree of hydrophobicity of xylan. Taking HPX (the least hydrophobic xylan) and APX3 (the most hydrophobic xylan) as an example, the difference in the water diffusivity is less than 20%. Further data analysis shows that this is because the increasing degree of hydrophobicity does not only decrease the degree of swelling of xylan but also decreases the number of polymer–water hydrogen bonds. The effect of swelling (decreasing water mobility) is offset by the effect of polymer–water hydrogen bonds (increasing water mobility). The observed differences in the swelling behavior between xylans with different degrees of hydrophobicity are due to the number of polymer–polymer hydrogen bonds being broken by water. There is a significant difference in the number of polymer–polymer hydrogen bonds being broken between the cases of HPX and APXs and such differences diminish as water concentration is increased. And most of the water molecules forming hydrogen bonds with xylans act as hydrogen bond acceptors rather than donors.

Acknowledgments

Funding from the NSERC Innovative Green Wood Fibre Products Network was greatly appreciated. The authors would also like to thank WestGrid and Compute/Calcul Canada for providing the computational facility and support for this research. We were grateful for data compilation work done by the summer student Amity Wong.

References

Ahlen, A. T. (1969). A study of the diffusion of sorbed water vapor through paper and regenerated cellulose films, Ph.D. thesis, The Institute of Paper Chemisty.
Cordeiro, N., Gouveia, C., Moraes, A., & Amico, S. (2011). Natural fibers characterization by inverse gas chromatography. *Carbohydrate Polymers*, *84*, 110–117.
Daura, X., Mark, A. E., & van Gunsteren, W. F. (1998). Parametrization of aliphatic CHn united atoms of gromos96 force field. *Journal of Computational Chemistry*, *19*(5), 535–547.
Ebringerova, A., & Heinze, T. (2000). Xylan and xylan derivatives - biopolymers with valuable properties, 1: naturally occurring xylans structures, isolation procedures and properties. *Macromolecular Rapid Communications*, *21*, 542–556.
Escalante, A., Goncalves, A., Bodin, A., Stepan, A., Sandstrom, C., Toriz, G., et al. (2012). Flexible oxygen barrier films from spruce xylan. *Carbohydrate Polymers*, *87*, 2381–2387.
Fundador, N. G. V., Enomoto-Roger, Y., TakemurA, A., & Iwata, T. (2012). Acetylation and characterization of xylan from hardwood kraft pulp. *Carbohydrate Polymers*, *87*, 170–176.
Gabrielii, I., & Gatenholm, P. (1998). Preparation and properties of hydrogels based on hemicellulose. *Journal of Applied Polymer Science*, *69*, 1661–1667.
Gennadios, A., Weller, C. L., & Testin, R. F. (1993). Modification of physical and barrier properties of edible wheat gluten-based films. *Cereal Chemistry*, *70*, 426–429.
Glasser, W. G., Jain, R. K., Sjostedt, M. A. (1995). Thermoplastic pentosan-rich polysaccharides from biomass, Tech. rep., 5430142 Finland/Rajamaki.
Goksu, E. I., Karamanlioglu, M., Bakir, U., Yilmaz, L., & Yilmazer, U. (2007). Production and characterization of films from cotton stalk xylan. *Journal of Agricultural and Food Chemistry*, *55*, 10685–10691.
Gonzalez, D., Santos, J., & Parajo, V. (2011). Manufacture of fibrous reinforcements for biocomposites and hemicellulosic oligomers from bamboo. *Chemical Engineering Journal*, *167*, 278–287.
Hansen, N. M. L., & Plackett, D. (2008). Sustainable films and coatings from hemicelluloses: A review. *Biomacromolecules*, *9*, 143–1505.
Hartman, J., Albertsson, A.-C., Lindblad, M. S., & Sjoberg, J. (2006). Oxygen barrier materials from renewable sources: Material properties of softwood hemicellulose-based films. *Journal of Applied Polymer Science*, *100*, 2985–2991.
Hockney, R. W., Goel, S. P., & Eastwood, J. W. (1974). Quiet high-resolution computer models of a plasma. *Journal of Computational Physics*, *14*(2), 148–158.
Hoover, W. G. (1985). Canonical dynamics: Equilibrium phase-space distributions. *Physical Review A*, *31*(3), 1695–1697.
Jain, R., Sjostedt, M., & Glasser, W. (2000). Thermoplastic xylan derivatives with propylene oxide. *Cellulose*, *7*, 319–336.
Mark, P., & Nilsson, L. (2001). Structure and dynamics of the tip3p, spc, and spc/e water models at 298 K. *Journal of Physical Chemistry A*, *105*(43), 9954–9960.
Mikkonen, K. S., & Tenkanen, M. (2012). Sustainable food-packaging materials based on future biore?nery products: Xylans and mannans. *Trends in Food Science and Technology*, *28*, 90–102.
Nose, S., & Klein, M. L. (1983). Constant pressure molecular-dynamics for molecular-systems. *Molecular Physics*, *50*(5), 1055–1076.
Nose, S. (1984). A molecular-dynamics method for simulations in the canonical ensemble. *Molecular Physics*, *52*(2), 255–268.
Pan, Y., Xiao, H., & Song, Z. (2013). Hydrophobic modification of cellulose fibres by cationic-modified polyacrylate latex with core-shell structure. *Cellulose*, *20*, 485–494.
Parrinello, M., & Rahman, A. (1981). Polymorphic transitions in single-crystalsa new molecular-dynamics method. *Journal of Applied Physics*, *52*(12), 7182–7190.
Peroval, C., Debeaufort, F., Despre, D., & Voillley, A. (2002). Edible arabinoxylan-based films. 1. Effects of lipid type on water vapor permeability, film structure, and other physical characteristics. *Journal of Agricultural and Food Chemistry*, *50*, 3977–3983.
Peura, M., Karppinen, T., Soovre, A., Salmi, A., & Tenkanen, M. (2008). Crystallization and shear modulus of a forming biopolymer film determined by in situ X-ray diffraction and ultrasound reflection methods. *Journal of Applied Physics*, *84*, 1371–1377.
Phan, T. D., Peroval, C., Debeaufort, F., Despre, D., Courthaudon, J. L., & Voilley, A. (2002). Arabinoxylan-lipids-based edible films and coatings. 2. Influence of sucroester nature on the emulsion structure and film properties. *Journal of Agriculture and Food Chemistry*, *50*, 266–272.
Pohjanlehto, H., Setala, H., Kammiovirta, K., & Harlin, A. (2011). The use of n, n'-diallylaldardiamides as cross-linkers in xylan derivatives-based hydrogels. *Carbohydrate Research*, *346*, 2736–2745.
Rauschenberg, N., Dhara, K., Palmer, J., & Glasser, W. (1990). Xylan derivatives from steam-exploded lignocellulosic resources-structure and properties. In *American Chemical Society, Polymer Preprints, Division of Polymer Chemistry*.
Saxena, A., Elder, T. J., & Ragauskas, A. J. (2008). Moisture barrier properties of xylan composite films. *Carbohydrate Polymers*, *104*, 023513(1–6).
Scott, W. R. P., Hunenberger, P. H., Tironi, I. G., Mark, A. E., Billeter, S. R., Fennen, J., Torda, A. E., Huber, T., Kruger, P., & van Gunsteren, W. F. (1999). The gromos biomolecular simulation program package. *Journal of Physical Chemistry A*, *103*(19), 3596–3607.
Shaikh, H., Pandare, K., Nair, G., & Varma, A. (2009). Utilization of sugarcane bagasse cellulose for producing cellulose acetates: Novel use of residual hemicellulose as plasticizer. *Carbohydrate Polymers*, *76*, 23–29.
Stepan, A. M., Hoije, A., Schols, H. A., de Waard, P., & Arabinose, G. P. (2012). content of arabinoxylans contributes to flexibility of acetylated arabinoxylan films. *Journal of Applied Polymer Science*, *125*, 2348–2355.
Sun, R., Sun, X., & Tomkinson, J. (2004). Hemicelluloses and their derivatives. *ACS Symposium Series*, *864*, 2–22.
Tanodekaew, S., Channasanon, S., & Uppanan, P. (2006). Xylan/polyvinyl alcohol blend and its performance as hydrogel. *Journal of Applied Polymer Science*, *100*, 1914–1918.
Theodorou, D. N., & Suter, U. W. (1985). Detailed molecular-structure of a vinyl polymer glass. *Macromolecules*, *18*(7), 1467–1478.
Voepel, J., Edlund, U., & Albertsson, A. (2009). Alkenyl-functlonalized precursors for renewable hydrogels design. *Journal of Polymer Science Part A: Polymer Chemistry*, *47*, 3595–3606.
Zhou, D. W., & Choi, P. (2012). Molecular dynamics study of water diffusivity at low concentrations in non-swollen and swollen polyurethanes. *Polymer*, *53*(15), 3253–3260.